Korean J. Chem. Eng., 36(5), 669-677 (2019)
DOI: 10.1007/s11814-019-0250-x

pISSN: 0256-1115
eISSN: 1975-7220

Flocculation kinetics and dewatering studies of quaternized cellulose derived from oil palm empty fruit bunches

Safia Syazana Mohtar*, Norasikin Saman*, Ahmad Mujahid Md Noor*, Tengku Nur Zulaikha Tengku Malim Busu*, Nor Aida Yusoff, and Hanapi Mat*,***,†**

*Advanced Materials and Process Engineering Laboratory, School of Chemical and Energy Engineering, Faculty of Engineering, Universiti Teknologi Malaysia, 81310 UTM Skudai, Johor, Malaysia
**Department of Chemical Engineering Technology, Faculty of Engineering Technology, Universiti Malaysia Perlis, Unicity Sg. Chuchuh Campus, 02100 Padang Besar, Perlis, Malaysia
***Advanced Materials and Separation Technologies (AMSET) Research Group, Health and Wellness Research Alliance, Universiti Teknologi Malaysia, 81310 UTM Skudai, Johor, Malaysia
(*Received 30 October 2018 • accepted 1 March 2019*)

Abstract−Flocculation kinetics and sludge dewatering of kaolin suspension as influenced by various q-EFBC flocculant dosing were studied. In this study, 62.5 mg L^{-1} q-EFBC exhibited the highest turbidity removal efficiency of 99.53± 0.08%. The adsorption rate of kaolin towards 12.5 mg L^{-1} to 112.5 mg L^{-1} q-EFBC dosing increased rapidly for t<60 s and became gradual before completion. The mass transfer coefficient was independent of dosage. The experimental data best-fitted the non-linear pseudo-first order due to the R^2>0.99 and the lowest standard deviation. The highest rate constant of particle aggregation and breakage was consistent with the highest rate constant of particle collision, which led to the highest turbidity removal at the optimal dosage. The rate-limiting steps in the flocculation process were particle collision and aggregation since their rate constant was lower than the other kinetic constants. The lower values of SRF and TTF of treated sludge as compared to the untreated one confirmed the improvement in the dewaterability characteristic. The lowest TTF (37.44±1.44 s) and SRF (1.49×10^{10} m kg^{-1}) was observed for 62.5 mg L^{-1} q-EFBC. The high turbidity removal and improved sludge dewaterability indicate the potential application of q-EFBC for water treatment.

Keywords: Adsorption, Flocculation, Kinetics, Cellulose, Turbidity Removal

INTRODUCTION

Fine particles in a suspension are commonly removed by the flocculation process through particle destabilization and agglomeration prior to sedimentation for disposal [1]. Due to the increasing awareness of sustainability and environmentally friendly concepts, the focus has been shifted towards developing environmentally friendly materials, such as natural-based flocculants like tamarind kernels [2], palm rachis [3], *Moringa oleifera*, *Opuntia ficus-indica* [4] and guar gum [5]. Cellulose, the most abundantly available polysaccharide, has also been studied concerning the isolation process from various sources (i.e., birch, date palm rachis and cotton) and modification with a range of chemicals to produce flocculants [3,6,7]. The excellent performance of cellulose-based flocculants in treating water and wastewater was proven; however, only limited reports on the flocculation kinetics of cellulose-based flocculants can be found in the literature [8-10].

In general, flocculation occurs after a considerable amount of added flocculants is adsorbed onto the suspended particles to initiate destabilization. The oppositely charged polymer molecules are attracted to the vacant particle surfaces, resulting in charge neutralization, forming bridges or patching [11]. In practical applications, the nature of flocculant adsorption on a particle surface and its reconformation are significant factors that determine the flocculation performance [11-13]. An initial adsorption process is rapid with numerous vacant surface sites, then, becomes slower before completion, resulting in the decrease of approachable unoccupied surface sites. The final quantity of adsorption, thus, depends on the available surface area of the system [12-14]. The adsorption of polymer then encourages agglomeration of flocs by colliding with one another, prompted by three possible modes of transport: a) Brownian motion; b) gradient velocity and c) differential sedimentation [13]. A dependable correlation between adsorption and flocculation processes can facilitate the control of flocculation, consequently enabling process-tuning aiming to attain the desired floc characteristics.

In conjunction with the flocculation process, sedimentation of fine particles is a subsequent common practice that produces a semi-solid slurry or sludge. The sludge is usually disposed of by composting, incineration and landfill, which faces challenging issues due to the cost (e.g., handling, transportation, and space) and management [15]. Therefore, an effective flocculation is required to minimize the sludge water content and volume, thus overcoming these issues. Sludge dewatering has been studied widely and several relevant review papers can be found in the literature discussing the types of flocculants [16], key parameters affecting sludge dewatering performance and characteristics [14,17,18], encountered challenges

†To whom correspondence should be addressed.
E-mail: hbmat@cheme.utm.my

and disposal techniques [15,19,20]. Over a decade, a number of biopolymer flocculants such as proteins, starch, chitosan, cellulose and lignin were reported [21-25]. These alternatives were developed to minimize the amount of synthetic flocculants in practical use or completely substituting them. They were usually modified through etherification or grafting in order to comply with the target pollutants charge, increase the molecular weight to enhance the flocculation stability and increase the water solubility for feasible application in various water treatment systems. Their application was unaided or used in combination with the commercially available flocculants, and some were reported to have superior performance over synthetic flocculants [21,23,25].

This study reports on the flocculation kinetics and the effect of the flocculation on the dewatering characteristics of producing sludge using a cellulose-based flocculant. The flocculant, quaternized cellulose (q-EFBC) derived from the oil palm empty fruit bunches (OPEFB), was used to remove turbidity of kaolin suspension by varying the dosage. The flocculation kinetics covered each flocculation stage, which includes adsorption of polymer onto particles and flocs formation. The adsorption process was studied based on the mass transfer and reaction-based kinetics models. Particle collision, aggregation and breakage were considered for aggregation kinetics of flocculation process. The dewatering characteristics of the generated sludge were assessed via the measurement of the time to filter (TTF) and specific resistance to filtration (SRF). The evaluation of each stage of the flocculation process up to the generation of sludge is necessary to better understand and predict the flocculation mechanisms as well as the effect of the flocculation process on the sludge dewatering properties.

MATERIALS AND METHODS

1. Materials

The q-EFBC used was OPEFB cellulose modified with 3-chloro-2-hydroxypropyl trimethylammonium chloride (degree of substitution (DS)=0.56; cellulose M_w=1,869 g mol^{-1}). The details of isolation, modification and characterization processes are described elsewhere [8,26]. Kaolin particles (average size: 5 μm, BET surface area: 14.18 m^2 g^{-1}, ρ: 2.4 g cm^{-3}) were purchased from Merck (Germany). The double-distilled water (DW) used throughout the experiments was produced using the AWS/4D Aquamatic Water Stills Hamilton (U.K.).

2. Flocculation Experiment

A jar test model VELP Scientifica JLT6 (Europe) equipped with six 75 mm×25 mm rectangular propellers was used to perform the flocculation process. A 300 mL of 1,400 mg L^{-1} kaolin suspension was prepared in DW and the pH of the suspension was adjusted to pH 7 using 0.1 M NaOH or HCl solution. The experiment was conducted by rapid stirring at 250 rpm for 3 min and slow stirring at 30 rpm for 30 min to promote the flocculation process. The flocs were allowed to settle down for 30 min prior to turbidity measurement using a Hanna instrument HI88703 Turbidimeter (Romania). The turbidity removal efficiency, ε_t (%) was calculated according to Eq. (1)

$$\varepsilon_t = \left(\frac{T_i - T_f}{T_i}\right) \times 100 \quad (1)$$

where T_i (NTU) and T_f (NTU) are the respective initial and final turbidity of the suspension.

The adsorption quantity, q (mg g^{-1}) of kaolin particles at varying q-EFBC dosages was determined by a depletion method. 2 mL of the suspension was taken at 15 s, 30 s, 45 s, 60 s, 120 s, 180 s, 600 s, 1,200 s and 1,800 s during slow stirring and filtered right away using a 0.45 μm nylon filter syringe. The residual concentration of the q-EFBC in the supernatant was determined by a high performance liquid chromatography (HPLC) model Agilent Technologies 1200 (U.S.A.) equipped with Rezex RPM-Monosaccharide column and RI detector (U.S.A.). The DW was used in the mobile phase with a flow rate of 0.6 mL min^{-1} at 60 °C. The q was calculated using Eq. (2)

$$q = \frac{(C_o - C_r) \times V}{m} \quad (2)$$

where C_o (mg L^{-1}) and C_r (mg L^{-1}) are the initial and residual concentrations of q-EFBC in the supernatant, respectively. V (L) is the volume of the suspension and m (g) is the mass of kaolin.

The flocculation degree was then monitored by measuring the kaolin concentration under slow stirring. The concentration was recorded and determined by a gravimetrical method at selected times, which were 15 s, 30 s, 45 s, 60 s, 120 s, 180 s, 600 s, 1,200 s and 1,800 s.

3. Filtration and Dewatering Experiments

The filtration and dewatering experiments were conducted continually using a 500 mL Buchner funnel (filter holder Ø=3.5 cm) equipped with an Edwards RV12 pump (England) and ACSI digital pressure meter (U.S.A.). The generated slurry after the flocculation process was poured into the filter under the pressure of 0.19 bars. The time at 25 mL of volume intervals was recorded. The filtration was prolonged for 5 min before the wet cake sample was collected and weighed. The wet cake was then dried at 105 °C until constant weight was reached. The wet and dried cake was weighed to determine moisture content (%) by Eq. (3)

$$\text{Moisture content (\%)} = \frac{\text{Weight of wet cake (g) - Weight of dry cake (g)}}{\text{Weight of wet cake (g)}} \times 100 \quad (3)$$

RESULTS AND DISCUSSIONS

1. Flocculation Kinetics

As a time dependent process, it is necessary to study the rate of kaolin adsorption for evaluating the flocculant performance in removing turbidity. In this study, a common approach of adsorption process was applied. Fig. 1 shows the q as a function of time t (s), for various q-EFBC dosages in kaolin suspension. It was found that the q increased rapidly at the early stage and became slower before completion. This could be explained by the numerous vacant active sites for adsorption at the beginning of the process. As the time increased, these unoccupied active sites decreased, subsequently completing the adsorption process. The increasing adsorption rate with q-EFBC dosage in this study was in agreement with Gregory and Barany [27]. However, eventually, saturation can occur and increasing dosage will no longer lead to an increase in adsorption

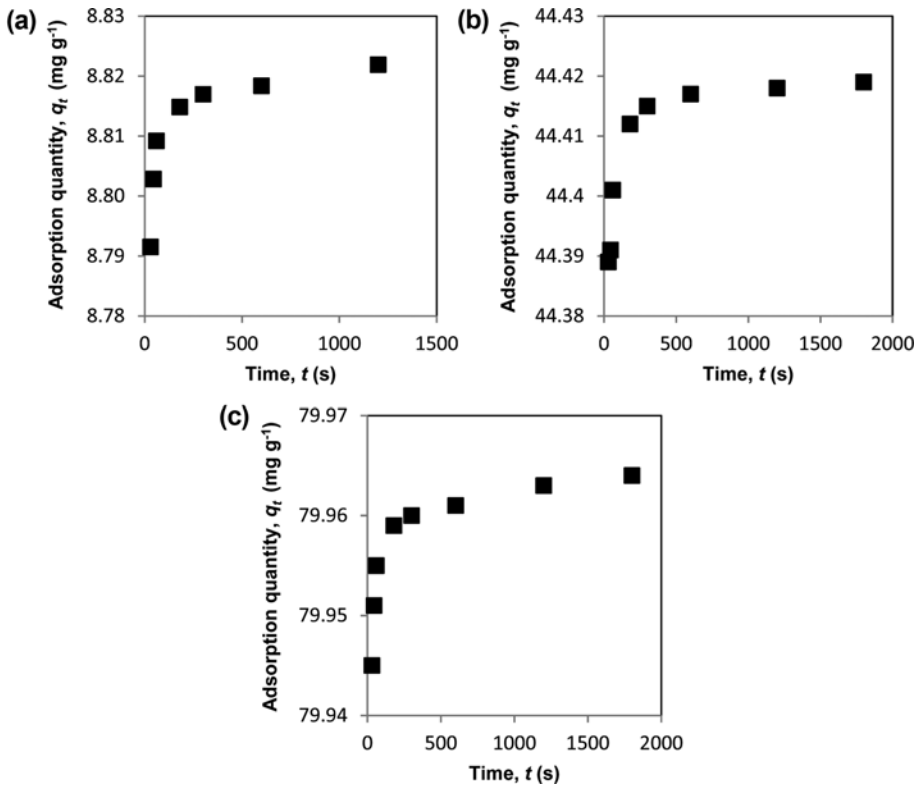

Fig. 1. Adsorption quantity versus time of (a) 12.5 mg L^{-1}, (b) 62.5 mg L^{-1} and (c) 112.5 mg L^{-1} q-EFBC dosage in kaolin suspension.

process [28].

The adsorption process was further investigated with an assumption that the flocculation process is described by four successive steps: 1) external mass transfer (transport of the flocculant molecules in bulk solution to the kaolin particles); 2) surface interaction on the kaolin particle; 3) rate of particles collision and 4) particles aggregation and breakage [12,29].

2. External Mass Transfer

The transport rate of the q-EFBC from the bulk solution to the suspended kaolin particles is studied by using the commonly used mass transfer model as shown in Eq. (4) [30]

$$V\frac{dC_t}{dt} = -mk_f S_s(C_t - C_s) \quad (4)$$

where V (m^3) is the volume of the particle-free liquid, C_t (mg L^{-1}) is the q-EFBC concentration at time t (s), m (g) is the mass of kaolin, k_f (cm s^{-1}) is the external mass transfer coefficient, S_s (m^2 g^{-1}) is the surface area of kaolin particle and C_s (mg L^{-1}) is the q-EFBC concentration at the external surface of the particle [30].

Assuming at t=0, $C_t=C_o$,

$$\left[\frac{d(C_t/C_0)}{dt}\right]_{t=0} = -\frac{m}{V}k_f S_s \quad (5)$$

The slope of $-k_f S_s$ was obtained from a plot of C_t/C_o versus t and the value of m/V is known; thus, k_f can be calculated and is presented in Table 1. The concentration of the q-EFBC in the suspension decreased with time. The effect of q-EFBC dosage was insignificant, in which, the transport rate for all dosages was fast

Table 1. Reaction-based kinetics models

Initial dosage (mg L^{-1})	12.5	62.5	112.5
Complete experimental adsorption quantity			
q_e (mg g^{-1})	8.85	44.42	79.58
External mass transport			
k_f (cm s^{-1})	3.35×10^{-4}	3.32×10^{-4}	3.35×10^{-4}
Non-linear PFO			
$q_{e,calc}$ (mg g^{-1})	8.86	44.40	79.58
k_1 (s^{-1})	0.18	0.32	0.46
R^2	0.99	0.99	0.99
SD (%)	0.03	8.00×10^{-3}	4.00×10^{-3}
Linear PFO			
$q_{e,calc}$ (mg g^{-1})	2.75	2.72	1.65
k_1 (s^{-1})	0.12	0.05	0.05
R^2	0.92	0.23	0.13
SD (%)	24.71	74.60	78.15
Non-linear PSO			
$q_{e,calc}$ (mg g^{-1})	8.92	44.41	79.59
k_2 (g mg^{-1} s^{-1})	0.11	1.60	0.81
R^2	0.99	0.98	0.99
SD (%)	1.18	0.01	0.02
Linear PSO			
$q_{e,calc}$ (mg g^{-1})	8.88	44.44	79.59
k_2 (g mg^{-1} s^{-1})	0.27	1.27	3.91
R^2	0.99	0.99	0.99
SD (%)	1.54	0.07	0.17

exceeding 98% in less than 15 s. The k_f values were found to be independent of the dosage.

3. Surface Interaction

The surface interaction between adsorbate (flocculant) and adsorbent (kaolin particles) can be described by several chemical reaction kinetic models. In this study, the non-linear and linear forms of pseudo-first order (PFO) and pseudo-second order (PSO) models were used. The equations are presented in Table 2. The validity of the models was determined by the coefficient of determination (R^2) and the standard deviation, SD (%) was calculated as in the following equation:

$$SD = \sqrt{\frac{\sum\left[\frac{q_{t,exp} - q_{t,cal}}{q_{t,exp}}\right]^2}{n-1}} \times 100 \quad (6)$$

where $q_{t,exp}$ and $q_{t,cal}$ are the respective experimental and calculation adsorption quantity at time t (s) and n is the number of data points.

The non-linear plots of PFO (NLPFO) and PSO (NLPSO) at various q-EFBC dosages are illustrated in Fig. 2. It was observed that although the R^2 value as presented in Table 1 for both non-linear models was close to 1, the SD value of NLPFO was the low-

Table 2. Turbidity removal efficiency, kinetic parameters and dewaterability characteristics of kaolin flocculation treated with a q-EFBC at various dosages

Kinetic models			Parameters	Eq.	Plot
PFO	Non-linear	$q_t = q_e(1-e^{-k_1 t})$	q_e (mg g^{-1}): complete adsorption quantity q_t (mg g^{-1}): adsorption quantity at time t (s)	(7)	q_t vs. t
	Linear	$\ln(q_e - q_t) = \ln q_1 - k_1 t$	q_1 (mg g^{-1}): calculated complete adsorption quantity k_1 (s^{-1}): PFO rate constant	(8)	$\ln(q_e - q_t)$ vs. t
PSO	Non-linear	$q_t = \frac{k_2 q_e^2 t}{1 + k_2 q_e t}$	k_2 (g mg^{-1} s^{-1}): PSO rate constant	(9)	q_t vs. t
	Linear	$\frac{t}{q_t} = \frac{1}{k_2 q_e^2} + \frac{t}{q_e}$		(10)	t/q_t vs. t

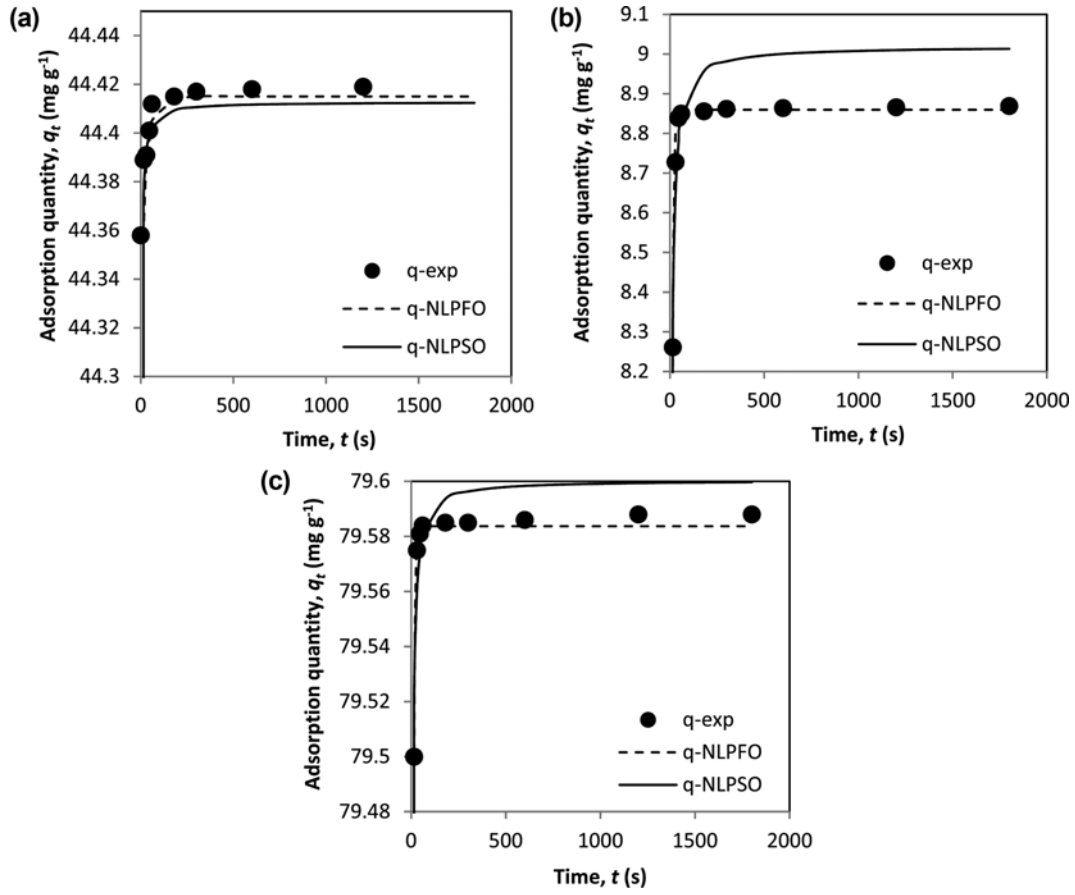

Fig. 2. Non-linear PFO and PSO models fitting for the adsorption of (a) 12.5 mg L^{-1}, (b) 62.5 mg L^{-1} and (c) 112.5 mg L^{-1} q-EFBC onto kaolin.

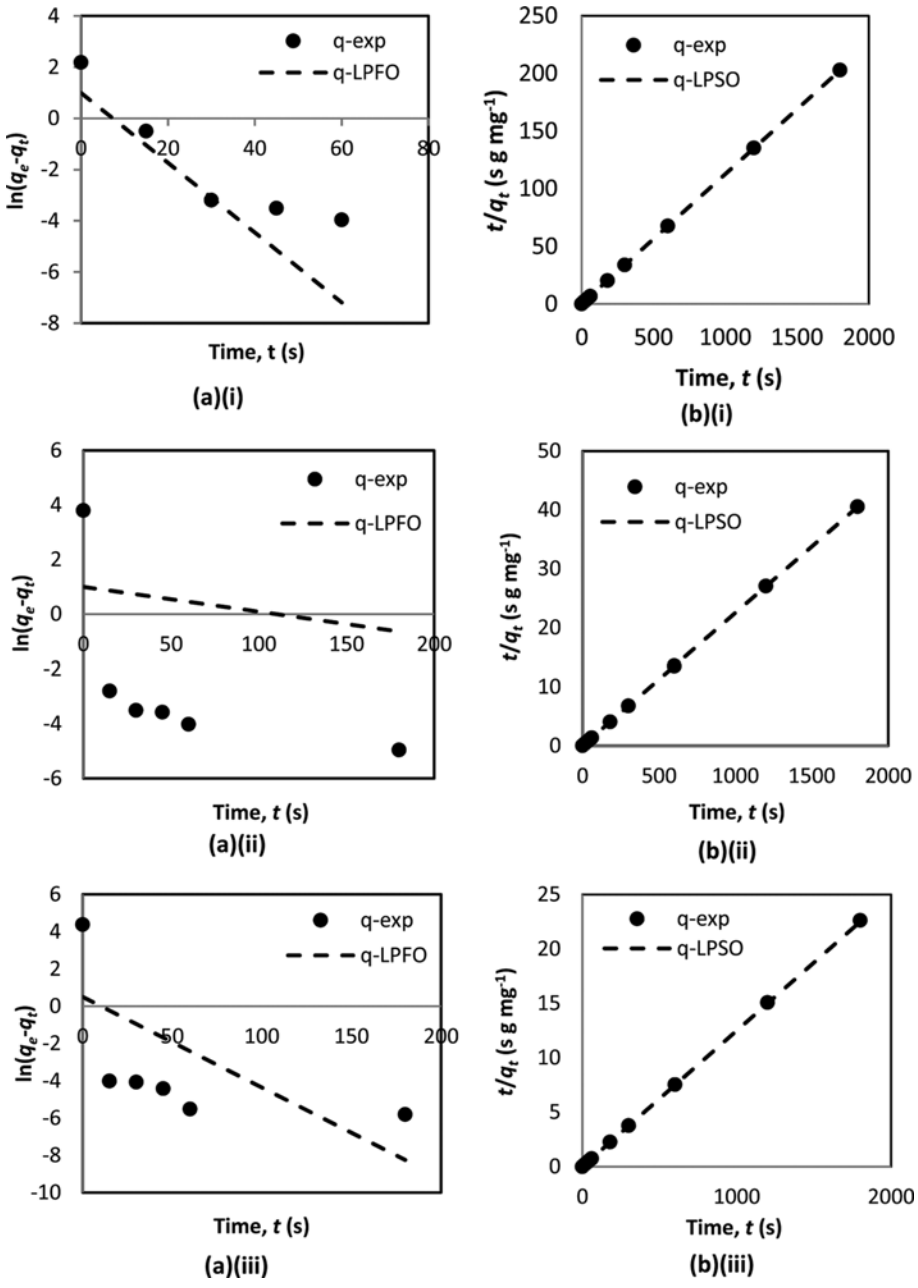

Fig. 3. Linear (a) PFO and (b) PSO models fitting for the adsorption of (i) 12.5 mg L^{-1}, (ii) 62.5 mg L^{-1} and (iii) 112.5 mg L^{-1} q-EFBC onto kaolin.

est. This indicates that the NLPFO was a better match kinetics model for the experimental data rather than the NLPSO. Further processing of the same experimental data by the linear PFO (LPFO) and PSO (LPSO), however, produced contradictory results. As shown in Fig. 3, the experimental data fit LPSO well with R^2 of 0.99 and a lower SD value as compared to LPFO. This contradiction, however, does not invalidate the decision of NLPFO as the best-fitted model to interpret the interaction between q-EFBC and kaolin particles at the surface since the deviation percentage was the lowest and the $q_{e,calc}$ was the closest to the experimental results. Moreover, several researchers recommended the use of a non-linear over linear form to describe the adsorption kinetics because linearization remarkably changed the units of x- and y-axis, thus altering the error distribution [31-33]. The k_1 of NLPFO as presented in Table 1 increased with q-EFBC dosage, which could be explained by the higher interaction of the flocculant molecules with the particle surface sites as the dosage increased. The increment in adsorption, however, is not indefinite as the saturation could occur at a higher flocculant dosage that no longer leads to the increase in adsorption [28,34,35].

4. Frequency of Particle Collisions

The collision of particles during flocculation was studied by determining the number of concentration, N (m^{-3}) reduction right after the rapid stirring ended, where t=0 s for 30 min with very

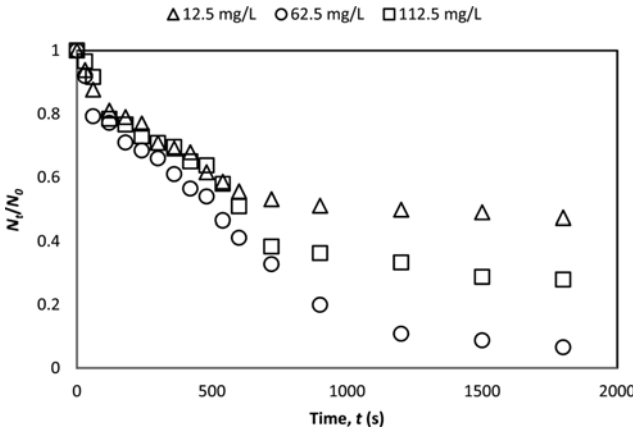

Fig. 4. A plot of N_t/N_o versus t for kaolin suspension at various q-EFBC dosages.

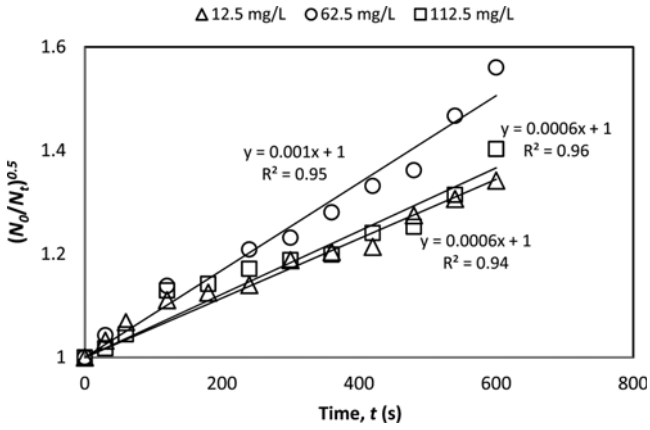

Fig. 5. A plot of $(N_o/N_t)^{0.5}$ versus t for kaolin suspension at various q-EFBC dosages.

slow stirring. The q-EFBC dosage was varied and the particle concentration was measured simultaneously by a gravimetrical method at specific times. Fig. 4 shows that the reduction of the N occurred considerably at the first 10 min, and thereafter the decrement became slower until t=30 min. The final concentration of the suspended kaolin particles was the lowest at q-EFBC dosage of 62.5 mg L^{-1} followed by 112.5 mg L^{-1} and 12.5 mg L^{-1}. This was expected since the 62.5 mg L^{-1} resulted in the highest removal of turbidity as shown in Table 3.

The change in N with time is due to the aggregation of particles into larger flocs. The highest N reduction at the earlier stage was found to be 112.5 mg L^{-1} q-EFBC. The N reduction, however, became slower than 62.5 mg L^{-1} dosage after 240 s, resulting the latter as the optimal dosage for the highest N reduction. On the other hand, the N reduction of 12.5 mg L^{-1} q-EFBC dosage was the lowest, reaching equilibrium at t=900 s. These results indicate that at a high flocculant dosage, after a certain time, an over equivalent adsorption of the positively charged flocculant would cause repulsion that would lead to a faster equilibrium as compared to the optimal dosage. Whereas, a low dosage is inadequate to fully flocculate the fine particles causing the fastest equilibrium.

The order of flocculation is mostly bimolecular; therefore, the frequency of particle collision is calculated using Eq. (11) [12]

$$\left(\frac{N_0}{N_t}\right)^{0.5}=1+\frac{1}{2}kN_0t \tag{11}$$

where k (m^3 s^{-1}) is the rate constant between single collisions. N_0 (m^{-3}) is the initial number of concentration and the calculated value is 5.39×10^{13} m^{-3} considering the known value of particle size (5 μm) and the initial kaolin density (2.4 g cm^{-3}). Similarly, N_t (m^{-3}), the number concentration of the kaolin particles at time t (s), can be calculated using the known particle's weight in a given time period, assuming that the portion of non-flocculated kaolin particles are singles [12,36]. The value of k as given in Table 3 was obtained from the slope of $(N_0/N_t)^{0.5}$ against t as shown in Fig. 5. The k of 62.5 mg L^{-1} q-EFBC dosage was found to be the highest, followed by 112.5 mg L^{-1} and 12.5 mg L^{-1} dosage. The highest k at an optimal q-EFBC dosage (62.5 mg L^{-1}) is attributed to the adequate accessibility of flocculant in the kaolin particle's vicinity. Sufficient amount of flocculant adsorbed onto kaolin surface causes mutual attraction among particles, increasing probability of collision. In addition, the larger agglomerated particles, if not settling, lead to a higher collision rate. At a lower dosage, the available flocculant molecules in the surrounding kaolin particles are scarce, resulting in a lesser collision. A higher dosage, conversely, causes rejection due to the saturation of flocculant molecules, thus reducing the collision of particles [28].

Table 3. Parameters of mass transfer and adsorption kinetics at various dosages

Initial dosage (mg L^{-1})	0 (Blank)	12.5	62.5	112.5
Turbidity removal efficiency				
ε_t (%)	57.33±1.22	90.70±0.66	99.53±0.08	98.02±0.04
Collision of particles				
k (m^3 s^{-1})	n/a	2.57×10^{-17}	4.31×10^{-17}	2.60×10^{-17}
Particles aggregation and breakage				
k_a (m^3 s^{-1})	n/a	7.79×10^{-17}	1.80×10^{-16}	7.29×10^{-17}
k_b (s^{-1})	n/a	2.10×10^{-3}	4.73×10^{-2}	1.50×10^{-3}
Sludge dewatering characteristics				
TTF (s)	101.40±1.27	58.97±6.59	37.00±1.44	48.06±5.77
SRF (m kg^{-1})	3.94×10^{10}	3.68×10^{10}	1.49×10^{10}	1.87×10^{10}

5. Particles Aggregation and Breakage

The flocs growth involves the formation and breakage so that the rate of aggregation is kept in balance. According to Jarvis et al. [37], aggregation of particles dominates over flocs breakage throughout the rapid initial formation of flocs. The significance of breakage increases until a steady-state floc size distribution is achieved. In this study, the aggregation of kaolin particles was studied based on the classical Smoluchowski model with the second-order kinetics of particle aggregation and the first-order kinetics aggregate breakage as shown in Eq. (12) [12]

$$\frac{d(N_t/N_0)}{dt} = -N_0 k_a \left(\frac{N_t}{N_0}\right)^2 + k_b \frac{N_t}{N_0} \tag{12}$$

where k_a ($m^3\ s^{-1}$) and k_b (s^{-1}) are the kinetic rate constants of particle aggregation and breakage, respectively.

Table 3 shows the rate constants, k_a and k_b, which were obtained from the plot of N_t/N_0 versus t as shown in Fig. 4. The k_a and k_b were first increased with dosage to an optimal value. This was encouraged by the increasing of q-EFBC acitve sites to facilitate more particle's interaction that brings about aggregation and breakage. Contrarily, further increment in dosing would only deteriorate the particle agglomeration because particle overcharging causes repulsion as observed for 112.5 mg L^{-1} dosage [12]. These results were in accordance to the collision of particles, in which, a higher possibility of collision leads to a higher aggregation as well as breakage. As the rate constant for particle collision and aggregation is extremely low as compared to the other rate constant, it suggests that the rate-limiting steps in flocculation process are the collision and aggregation of particles.

6. Sludge Dewatering Characteristics

The removal of turbidity in the kaolin suspension depends on the dosage of the flocculants used. In this study, q-EFBC has an optimum dosage of 62.5 mg L^{-1} for the highest turbidity removal as shown in Table 3. This is expected since too low a dosage is inadequate for particle agglomeration and the excess dosage could cause redispersion of the agglomerated particles. Most water treatment plants generate large quantities of sludge produced from the flocculation and filtration processes. The characteristics of sludge dewaterability, therefore, were evaluated through the measurement of TTF and SRF at various q-EFBC dosages. The TTF in this study defines the required time to collect 50 mL of filtrate. The TTF, as shown in Table 3, initially decreased with the increased dosage, reached the lowest at 62.5 mg L^{-1} q-EFBC, then increased slightly at 112.5 mg L^{-1} q-EFBC. These values were lower than that of the TTF for kaolin dispersion without treatment (blank), which confirms the improvement in sludge dewatering characteristics by q-EFBC.

The SRF was calculated using the following Eq. (13) to (17) [38]:

$$\frac{t}{V} = \frac{\mu\beta}{2PA^2K}V + \frac{\mu R_m}{AP} \tag{13}$$

where t (s) is the time of filtrate volume V (m^3), μ (N s m^{-2}) is the fluid viscosity, P (N m^{-2}) is the applied pressure during the filtration, A (m^2) is the filter area, K (m^2) is the cake permeability, R_m (m^{-1}) is the medium resistance, and β is the volume ratio of cake to filtrate as given by Eq. (14)

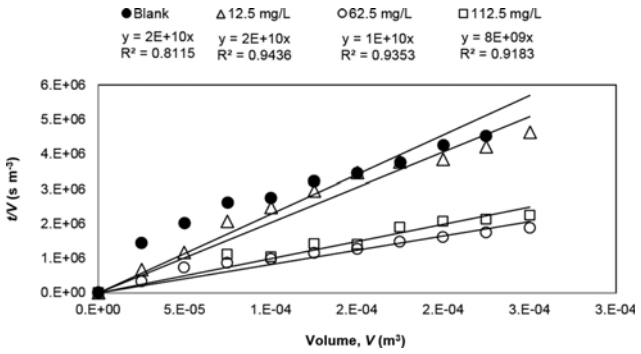

Fig. 6. A plot of t/V versus V for kaolin suspension dewatering at various q-EFBC dosages.

$$\beta = \frac{\rho_1 s}{(1-s)C\rho_s - (1-C)\rho_1 s} \tag{14}$$

where s is the mass fraction of solid in the slurry, ρ_1 (kg m^{-3}) and ρ_2 (kg m^{-3}) are the liquid and solid densities, respectively, and C is the cake concentration by volume fraction as given by Eq. (15).

$$C = \frac{\dfrac{\text{dry cake weight}}{\text{solid density}}}{\dfrac{\text{dry cake weight}}{\text{solid density}} + \dfrac{\text{moisture in weight cake}}{\text{water density}}} \tag{15}$$

The slope of the plot of t/V versus V was used to calculate the cake permeability, K (m^2) using Eq. (16)

$$K = \frac{\mu\beta}{2PA^2b} \tag{16}$$

where b (s m^{-6}) is the slope of the t/V versus V. The SRF (m kg^{-1}) was determined by Eq. (17).

$$SRF = \frac{1}{KC\rho_s} \tag{17}$$

As shown in Fig. 6, the slope, b, of 112.5 mg L^{-1} and 62.5 mg L^{-1} was lower than the blank, indicating a faster time taken for water separation. The SRF value for both dosage was comparable. The SRF of 12.5 mg L^{-1}, on the other hand was higher and almost equivalent to the blank. This indicates that too low a q-EFBC dosage was unable to assist the dewatering process.

The lowest TTF and SRF values obtained at an optimal dosage implies that an adequate amount of q-EFBC enhanced sedimentation by producing larger and heavier flocs, thus improving the sludge dewaterability characteristic. In an ideal situation, the hydration shell of sludge can be destroyed by the interaction between the opposite charges of particles and flocculant [23]. The charge neutralization of the positively charged q-EFBC and the negatively charged kaolin diminished the surface tension of water, reduced gradually the thickness of the hydration shell. This prompted the release of more bound water into the sludge bulk solution, thus resulting in a better dewatering performance [39]. Inadequate q-EFBC dosage of 12.5 mg L^{-1} has a weaker charge neutralization, which explains the highest TTF and SRF values. On the other hand, an excess q-EFBC generated repulsive force and restabilized the suspension [16]. This explains a slight increment of TTF and SRF

Table 4. Cost estimation of q-EFBC

Materials	Price (USD/tonne)	Quantity (g)	Cost (USD)
OPEFB	250.00	2.00	1.00×10^{-3}
[bmim][Cl]	100000.00	20.00	[a]0.67
Acetone	2000.00	156.80	[a]0.11
NaOH	500.00	3.51	2.00×10^{-3}
Urea	300.00	3.51	1.00×10^{-3}
Thiourea	1400.00	2.86	4.00×10^{-3}
CHPTAC	1300.00	16.96	0.02
Total cost (USD g^{-1})			0.80
Polyacrylamide (USD g^{-1})			3.00×10^{-3}
Aluminium sulfate (USD g^{-1})			2.00×10^{-4}

[a]Estimated price for three cycles of isolation process

on 112.5 mg L^{-1} q-EFBC. In addition, for an organic polymer flocculant such as q-EFBC, increasing the dosage only increases the water viscosity and deteriorates the dewatering performance even more [16].

7. Mechanism of Flocculation Process

In this study, the flocculation mechanism of q-EFBC flocculant in kaolin suspensions is explained by means of the kinetics approach. This involves an adsorption of flocculant onto particles and floc formation. During flocculation, the flocculant molecule is transferred to the particle surface at its respective rate from bulk solution and the interaction on the particle surface occurs right after. For polyelectrolyte such as q-EFBC, the interaction can be studied by means of zeta potential. The initial zeta potential of kaolin suspension was −22.31 mV. Since the positively charged q-EFBC molecule was strongly attracted to the negatively charged kaolin particle, the zeta potential value increased with dosage. At an optimal dosage, the zeta potential was −1.04 mV, which was the closest value to 0 mV. This was expected since an adequate attachment of the flocculants onto the kaolin particles neutralizes the charge, attaining an isoelectrical point of zeta potential (0 mV), largely eliminating the repulsion force among particles, thus subsequently initiating destabilization of the suspension [13]. For lower dosage of q-EFBC, the zeta potential was −7.10 mV. Although this is able to achieve 92% turbidity removal efficiency, the zeta potential value, which inclined to the negative site indicates that a low flocculant dosage was insufficient for an effective destabilization. On the other hand, at 112 mg L^{-1}, the zeta potential value of 3.84 mV indicates that a high dosage could compensate the negativity of the kaolin particles and inclined to a positive site. It is expected that an excess of flocculant dosage would increase the zeta potential value until adsorption is completed and causes rejection for aggregation due to the overcharging.

Flocculation subsequently takes place after particle destabilization. After the adsorption process, the flocculant (q-EFBC) would attach to two or more kaolin particles encouraged by the collisions between particle-particle, particle-floc and floc-floc due to slow fluid motion, then forming polymer bridges. The floc growth is dominated by aggregation. Since the aggregation occurs under stirring, the breakage of particles was common and in this study, based on the obtained kinetic data, the breakage increased with the floc growth. As shown in Tables 1 and 3, 62.5 mg L^{-1} q-EFBC resulted in the highest turbidity removal, regardless of the highest q of 112.5 mg L^{-1} q-EFBC. The particle collision frequency seems to be the key to remove suspended kaolin particle successfully using q-EFBC since the rate was the highest and resulted in the highest aggregate coefficient.

8. Economic Analysis

For practical use, the rough estimated cost of q-EFBC with 1 g q-EFBC as a basis is presented in Table 4. The cost for an optimal flocculant dosage was much higher than the commercially available polyacrylamide and aluminium sulfate. About 96% of the total cost was derived from the cellulose isolation process, which used as ionic liquid (1-butyl-3-methyl imidazolium chloride, [bmim][Cl]) and acetone, as reported in Mohtar et al. [26]. Although the three times recyclability was considered in the estimation, the price was still high. The estimated cost, if excluding the pricey isolation process, was approximately USD 0.03. Even though the price is still high, considering the advantages of natural biopolymers towards human and environmental benefits, the application of cellulose as a flocculant should be taken into account. It is suggested that more economical isolation should be applied to make the application practicable.

CONCLUSION

The flocculation kinetics and sludge dewaterability of kaolin suspension treated with q-EFBC are affected by the initial flocculant dosage. Merely sufficient amount of q-EFBC could effectively destabilize the suspension, which occurs at an isoelectrical point of zeta potential, subsequently flocculating to form larger and heavier flocs for easier filtration. The adsorption quantity increases with dosage, and the rate increases rapidly at first before decreasing gradually towards completion. The highest rate constant of collision and aggregation at the optimal dosage, indicates that an effective flocs formation ensues after particle collisions and aggregation regardless of a reasonable particle breakage. The q-EFBC improved the sludge dewaterability by reducing the TTF and SRF, with the lowest at the optimal q-EFBC dosage. The estimated cost of the q-EFBC was higher than the commercially available flocculants/coagulants due to the pricey isolation process. Thus, a more economical

isolation process should be introduced considering the advantages offered by this natural-based polymer to humans and the environment.

ACKNOWLEDGEMENTS

We gratefully acknowledge financial support from the Ministry of Science, Technology and Innovation, Malaysia under the eScience Research Program (Project No. 4S071); the Universiti Teknologi Malaysia (UTM) under the Research University Grant (Project No. 06H85); technical supports from the Syarikat Air Johor Sdn. Bhd. and Indah Water Konsortium Berhad; MyBrain15 scholarship from the Ministry of Higher Education (Malaysia); and UTM Postdoctoral Fellowship Scheme (PDRU, 03E92 and 04E29) awarded to Safia Syazana Mohtar and Norasikin Saman.

REFERENCES

1. R. Hogg, *Int. J. Miner. Process.*, **58**, 223 (2000).
2. G. Pal, S. Sen, S. Ghosh and R. P. Singh, *Carbohyd. Polym.*, **87**, 336 (2012).
3. R. Khiari, S. Dridi-Dhaouadi, C. Aguir and M. F. Mhenni, *J. Environ. Sci.*, **22**, 1539 (2010).
4. J. Beltrán-Heredia and J. Sánchez-Martín, *J. Hazard. Mater.*, **164**, 713 (2009).
5. J. Tripathy, D. K. Mishra, A. Srivastava, M. M. Mishra and K. Behari, *Carbohyd. Polym.*, **72**, 462 (2008).
6. H. Liimatainen, J. Sirviö, O. Sundman, M. Visanko, O. Hormi and J. Niinimäki, *Bioresour. Technol.*, **102**, 9626 (2011).
7. Y. Song, J. Zhang, W. Gan, J. Zhou and L. Zhang, *Ind. Eng. Chem. Res.*, **49**, 1242 (2010).
8. S. S. Mohtar, T. N. Z. Tengku Malim Busu, A. M. Md. Noor, N. Shaari, N. A. Yusoff, M. A. Che Yunus and H. Mat, *Clean Technol. Environ.*, **19**, 191 (2017).
9. H. Kono, *Resour. Eff. Technol.*, **3**, 55 (2017).
10. Z. Yang, K. Ren, E. Guibal, S. Jia, J. Shen, X. Zhang and W. Yang, *Chemosphere*, **161**, 482 (2016).
11. M. G. Rasteiro, I. Pinheiro, H. Ahmadloo, D. Hunkeler, F. A. P. Garcia, P. Ferreira and C. Wandrey, *Chem. Eng. Res. Des.*, **95**, 298 (2015).
12. Y. Chen, S. Liu and G. Wang, *Chem. Eng. J.*, **133**, 325 (2007).
13. J. Gregory, in: Encyclopedia of colloid and interface science, T. Tadros (Ed.), Springer, Berlin, Heidelberg (2013).
14. C. Ding, Y. Li, Y. Wang, J. Li, Y. Sun, Y. Lin, W. Sun and C. Luo, *Int. J. Biol. Macromol.*, **107**, 957 (2018).
15. M. Kacprzak, E. Neczaj, K. Fijałkowski, A. Grobelak, A. Grosser, M. Worwag, A. Rorat, H. Brattebo, Å. Almås and B. R. Singh, *Environ. Res.*, **156**, 39 (2017).
16. H. Wei, B. Gao, J. Ren, A. Li and H. Yang, *Water Res.*, **143**, 608 (2018).
17. M. L. Christensen, K. Keiding, P. H. Nielsen and M. K. Jørgensen, *Water Res.*, **82**, 14 (2015).
18. Y. Qi, K. B. Thapa and A. F. A. Hoadley, *Chem. Eng. J.*, **171**, 373 (2011).
19. P. -A. Tuan, S. Mika and I. Pirjo, *Drying Technol.*, **30**, 691 (2012).
20. V. H. P. To, T. V. Nguyen, S. Vigneswaran and H. H. Ngo, *Water Sci. Technol.*, **74**, 1 (2016).
21. B. T. Liu, H. Y. Song and Y. X. Li, *Adv. Mater. Res.*, **383**, 3134 (2012).
22. L. Kuutti, S. Haavisto, S. Hyvarinen, H. Mikkonen, R. Koski, S. Peltonen, T. Suortti and H. Kyllönen, *Bioresources*, **6**, 2836 (2011).
23. J.-P. Wang, S.-J. Yuan, Y. Wang and H.-Q. Yu, *Water Res.*, **47**, 2643 (2013).
24. T. Suopajärvi, J.-A. Sirviö and H. Liimatainen, *J. Environ. Chem. Eng.*, **5**, 86 (2017).
25. K. Zhou, J. Stüber, R.-L. Schubert, C. Kabbe and M. Barjenbruch, *Water Sci. Technol.*, **77**, 7 (2017).
26. S. S. Mohtar, T. N. Z. Tengku Malim Busu, A. M. Md Noor, N. Shaari and H. Mat, *Carbohyd. Polym.*, **166**, 291 (2017).
27. J. Gregory and S. Barany, *Adv. Colloid Interface Sci.*, **169**, 1 (2011).
28. M. Hema and S. Arivoli, *J. Appl. Sci. Environ. Manage.*, **12**, 43 (2008).
29. N. Saman, K. Johari, S.-T. Song, H. Kong, S.-C. Cheu and H. Mat, *J. Environ. Chem. Eng.*, **4**, 2487 (2016).
30. R. Ocampo-Perez, R. Leyva-Ramos, P. Alonso-Davila, J. Rivera-Utrilla and M. Sanchez-Polo, *Chem. Eng. J.*, **165**, 133 (2010).
31. H. N. Tran, S.-J. You, A. Hosseini-Bandegharaei and H.-P. Chao, *Water Res.*, **120**, 88 (2017).
32. C. P. Bergmann and F. Machado, Carbon nanomaterials as adsorbents for environmental and biological applications, Springer International Publishing, Switzerland (2015).
33. K. V. Kumar, *J. Hazard. Mater.*, **137**, 1538 (2006).
34. W. Lick, Sediment and contaminant transport in surface waters, CRC Press, Boca Raton (2009).
35. J. Gregory, Particles in water: Properties and processes, CRC Press, Boca Raton (2006).
36. K. K. Das and P. Somasundaran, *J. Colloid Interface Sci.*, **271**, 102 (2004).
37. P. Jarvis, B. Jefferson and S. A. Parsons, *Rev. Environ. Sci. Biotechnol.*, **4**, 1 (2005).
38. L. Besra, D. K. Sengupta and S. K. Roy, *Int. J. Miner. Process.*, **59**, 89 (2000).
39. H.-F. Wang, H. Hu, H.-J. Wang and R. J. Zeng, *Sci. Total Environ.*, **643**, 1065 (2018).